

Tacrine-allyl/propargylcysteine-benzothiazole trihybrids as potential anti-Alzheimer's drug candidates

Asha Hiremathad,^{a,b} Karam Chand,^a A. Raquel Esteves,^c Sandra M. Cardoso,^{c,d}
Rona R. Ramsay,^e Sílvia Chaves^a, Rangappa S. Keri,^{b,*} M. Amélia Santos^{a,*}

^a *Centro de Química Estrutural, Instituto Superior Técnico, Universidade de Lisboa, Av. Rovisco Pais 1, 1049-001 Lisboa, Portugal.*

^b *Centre for Nano and Material Sciences, Jain University, Jain Global Campus, Bangalore, Karnataka, 562112, India.*

^c *CNBC – Centro de Neurociências e Biologia Celular, Universidade de Coimbra, Coimbra, Portugal.*

^d *Faculdade de Medicina, Universidade de Coimbra, 3030 Coimbra, Portugal.*

^e *Biomedical Sciences Research Complex, University of St Andrews, Biomolecular Sciences Building, North Haugh, St Andrews KY16 9ST, UK.*

Keywords: Alzheimer's disease; Trihybrid drugs; Tacrine; Anti-A β aggregation; MAO-B; Anti-neurodegeneration

*

Corresponding Authors:

[†]For M.A.S.: phone, +351-218419273; email, masantos@ist.utl.pt

[‡]For K.S.R.: phone, +91-8027577199; email, keriphd@gmail.com

Abstract

On continuing our research on new drug candidates for Alzheimer's disease (AD), we have designed, synthesized and evaluated a series of multifunctional trihybrid agents. The design strategy was based on the incorporation of a benzothiazole (BTA) moiety on a series of very recently reported bihybrids, resulting from the conjugation of a tacrine (TAC) with natural based moieties, namely S-allylcysteine (SAC) (garlic constituent) and S-propargylcysteine (SPRC). Thus, in addition to the acetylcholinesterase inhibition (AChEI) and anti-ROS capacity of the bihybrids (TAC-SAC/SPRC), the new trihybrids (TAC-SAC/SPRC-BTA) appeared endowed with 5-fold capacity for inhibition of the amyloid beta-peptide (A β 3) aggregation. The BTA moiety led also to considerable enhancement of the AChEI on the trihybrids, which molecular modeling suggested as being due to the simultaneous binding to the catalytic active site and peripheral anionic site of AChE. The trihybrids were also assessed for the MAO inhibition, but resulted in lower activity than expected, ascribed to the low accessibility of the propargyl groups to the enzyme active site. Finally, the effects of the compounds on the viability of neuroblastoma cells stressed with A β 3⁴² and H₂O₂ showed moderate cell protection. Overall, the performed studies illustrate the importance (and limitations) of enclosing several molecular scaffolds in one molecular entity to allow the modulation of multiple AD targets.

1. Introduction

Alzheimer's disease (AD) is one of the most devastating age-related neurodegenerative disorders with no cure so far, characterized by progressive memory loss and other cognitive impairments. The increase of life expectancy of humans and the exponential rise in the number of cases of AD support the need for developing an effective treatment for this frontline health problem.¹ Although its etiology has not been yet well understood, the patient brains are characterized by A β 3-amyloid (A β 3) deposits (plaques) around neurons and neurofibrillary tangles (NFT) inside neurons,² increased oxidative stress and disruption of metal homeostasis.³ Other prominent features of AD are disturbances in neurotransmitters, especially acetylcholine (cholinergic) deficit due to its hydrolysis by

acetylcholinesterase (AChE). Since around two decades ago, AD patients have been mainly treated with inhibitors of AChE (AChEI), but with limited therapeutic success. In fact they can provide amelioration of symptoms (improving patient memory) for a limited time window and for mild situations, but cannot alter the course of the disease.⁴ The multifactorial nature and the complexity of AD is believed to be the main reason for the absence of effective drugs, and has led to the emergence of multitargeting drugs. Under this approach, one molecular entity is conveniently polyfunctionalized to enable its simultaneous binding interaction with several of the most important targets, but mostly focused on inhibition of AChE and A β -aggregation and/or on the control of the brain oxidative stress.⁵ Monoamine oxidase (MAO) has also been considered an important target for the treatment of AD,⁶ since it catalyzes the oxidative deamination of the monoamine based neurotransmitters, such as serotonin and dopamine, with the concomitant production of H₂O₂ that can promote the Fenton reaction and formation of reactive oxygen species (ROS).⁷

In this context, the development of multitargeting drugs for treatment of AD has been a challenge for many research groups.^{8,9,10} Most of the multitarget drug design strategies have been driven by the recognized importance of maintaining the cholinergic functions (cholinergic hypothesis). Thus, they include a main molecular framework based on approved anti-AD drugs (AChE inhibitors), which is modified (hybridized) with other functional units to hit other disease targets. Among the USA FDA anti-AD drugs that are AChEI (e.g. tacrine, donepezil, rivastigmine, and galanthamine),¹¹ tacrine was the first and most potent AChEI (discontinued due to side effects such as hepatotoxicity),¹² with superiority in the structural modification, thus making it a privileged structure for incorporation into the overall molecular skeletons of the multi-target-directed drugs for the treatment of AD.¹³ In fact, we can find tacrine hybrids containing fragments of donepezil or galanthamine, while also a number of hybrids containing a structural fragment derived from natural based products such as alkaloids, flavonoids or others.

An important part of our current research has also been a focus on the development of acetylcholine esterase inhibitors functionalized for the inhibition/modulation of other AD targets, namely A β aggregation, oxidative stress and redox-active metal ions.^{14,15,16} Very recently, the conjugation of tacrine (TAC) with S-allylcysteine (SAC) and S-

propargylcysteine (SPRC), two natural based products with neuroprotective and antioxidant roles (e.g. garlic derivatives),^{17,18} resulted in a set of bihybrids (TAC-SAC and TAC-SPRC) with important neuroprotecting properties which, besides the expected AChEI and anti-oxidant properties, presented also inhibitory activity for the self- and Cu-induced A β aggregation.^{19,20} Interestingly, N-propargylamine is also an important pharmacophore used in the design of MAO inhibitors.^{8,21} In this work we report the design, synthesis and biological evaluation of a new set of trihybrids (see Fig. 1) which,

Insert here Fig 1

in addition to the functional groups presented in the above bihybrids, include also a benzothiazole (BTA) moiety to enhance the inhibition of A β aggregation, since BTA is a derivative of thioflavine T (ThT), a well known A β dye widely used in the design of AD drugs.^{14,22} Furthermore this new set of eight hybrids was designed by selection of suitable linkers to enable a dual mode binding, via the tacrine and BTA moieties, with both active binding sites of AChE. Besides the description of the design and synthetic procedures, we include herein the results and discussion of the bioassays, namely the inhibition of AChE, A β aggregation, MAOs and anti-oxidant properties, as well as their effect on the neuronal cell viability upon being subjected to model stressors of AD.

2. Results and Discussions

2.1 Molecular design and modeling

The design of the new trihybrids, to be subsequently prepared and studied (Fig. 2), involved a preliminary selection of the three molecular scaffolds, to address for main biological symptoms associated with AD, and then docking simulations were carried out to set the optimal length of the linker between the main frameworks.

Insert here Fig 2

The selection of the main molecular moieties was based on our previous works, specifically: tacrine (TAC) and the natural based S-allylcysteine (SAC) or S-propargylcysteine (SPRC) to endow the hybrids with anti-AChE and anti-oxidant properties;¹⁹ benzothiazole (BTA) to promote the interaction with A β and anti-A β aggregation properties; on the other hand, an adequate linkage of TAC with BTA to warrant a dual binding mode within the active site of AChE and increase the enzymatic

inhibition.¹⁴ Based on previous studies, an alkyl-amide linker could avoid linker strain and the length was selected based on docking simulation of the ligand into the enzyme, TcAChE. These studies also explained the interaction modes of the trihybrids with AChE. Preliminary docking results showed that three to five methylenes could provide the linker with adequate length to enable the dual mode interaction with the two molecular fragments (TAC, BTA) within the AChE gorge. A more detailed analysis of the simulation results shows that the trihybrids could simultaneously bind to both the catalytic anionic site (CAS) and the peripheral anionic site (PAS) (see representative results of the docking studies in Fig 3).

Insert here Fig 3

The tacrine appears inserted in the bottom of the enzyme gorge, adopting a parallel *n-n* stacking interaction with Trp84 and Phe330 of CAS, and blocking the accessibility of substrate and water to the active site (formed by the “catalytic triad” Ser200, His440 and Glu327);²³ The benzothiazole moiety occupies the PAS having a *n-n* interaction with Trp279 and Tyr70. The structure found for these hybrid-enzyme complex models is quite similar to the reported crystal structure of TcAChE complexed with a tacrine-quinoline inhibitor (N-4'-quinolyl-N'-9''-(1'',2'',3'',4''-tetrahydroacridinyl)-1,8-diaminooctane; PDB entry 1ODC),²⁴ as shown for **10g** (Fig. 3A). These simulations also indicated the capacity of the linker amide group to establish H-bond interactions between its NH and the phenolic group of Tyr121. Interestingly, in opposition to the observed previously for the corresponding bihybrids (TAC-SAC and TAC-SPRC),¹⁹ all the trihybrids could accommodate the allyl and propargyl groups outwards the lipophilic part of PAS, which is left free for the stronger interaction with the BTA moiety. Furthermore, these allyl and propargyl groups do not seem to result in considerable differences on the ligand-enzyme interaction (see Fig.3B for **10c** and **10g**). These simulations also illustrate that compounds with longer chains (n = 5), as **10b**, have the BTA moiety slightly shifted outwards the PAS aromatic residues, which may result in somehow lower *n-n* interaction with this site than the shorter compounds (n = 3), as **10a** (see Fig. 3C). Lastly, although 6-chloro-tacrine is known for its higher activity, as compared with the corresponding tacrine derivatives, this was not clearly evidenced from the docking results, namely superimposition of **10c** and **10a** (see Fig. 3D). Notably, this chloro atom (green coloured) appears to be well

accommodated in close distance of Hist440, which is thought to be the rationale for that enhancement on inhibitory activity, namely due to an H-bond interaction between its carbonyl oxygen and the tacrine pyridinium group.²⁵

Overall, the modeling studies give some support to the expected ability of the trihybrids to interact with both the CAS and PAS of AChE, thus explaining some of the stronger calculated inhibitory activities, as compared with the corresponding bihybrids. However, since the binding modes found for these compounds were so similar to each other, their relative potency as inhibitors would be difficult to predict with confidence.

2.2 Chemistry

The designed tacrine-*S*-allylcysteine-benzothiazole (TAC-SAC-BTA) and tacrine-*S*-propargylcysteine-benzothiazole (TAC-SPRC-BTA) hybrids were synthesized according to a convergent synthetic approach shown in Scheme 1. The 9-chloro-1,2,3,4-tetrahydroacridine (**3**) was prepared from commercially available anthranilic acid as previously reported.^{26,27} Amino alkyl acids were attached to the **3a** and **3b**, using a catalytic amount of KI and phenol to obtain the intermediates 2-(1,2,3,4-tetrahydroacridine-9-ylamino) acids **4(a-d)**. The synthesis of the BTA-cysteine intermediates **9(a,b)** involved four steps: firstly, L-cysteine (**5**) was *S*-alkylated with allyl bromide and propargyl bromide in the presence of NH₄OH to yield the 3-allylsulfanyl-2-amino-propionic acid (**6a**) and 2-amino-3-prop-ynylsulfanyl-propionic acid (**6b**), respectively; their amino group was Boc-protected by reaction with di-*tert*-butyl dicarbonate (Boc) to yield compounds **7(a,b)**; these compounds were coupled with a BTA unit, through the condensation of the benzothiazole-2-amine (**8**) to their carboxylic group (T₃P-activated), and subsequently the *Boc* group was released from the amine group with TFA to obtain the intermediates **9(a,b)**. Lastly the condensation of both intermediate compounds **4(a-d)** and **9(a,b)** in the presence of T₃P and NMM afforded the ultimate novel hybrids **10(a-h)**.

Insert here Scheme 1

2.3. Biological activity

2.3.1. AChE inhibition

TcAChE enzymatic inhibition by the newly synthesized compounds **10(a-h)** was evaluated by adaptation of a method previously described.¹⁵ The IC_{50} values for AChE inhibition are depicted in Table 1 (see also data plots in Fig. S9). These series of compounds showed inhibitory activity in submicromolar range, even slightly better than the standard drug (tacrine). Among those, as we expected, the compounds with the chloro-substituted tacrine moiety showed higher inhibition ($IC_{50} = 0.25-0.28$ μ M), with no considerable difference between the propargyl/allyl cysteine substituents. Overall, the compound with chlorotacrine and *S*-propargylcysteine groups (**10g**) showed highest AChE inhibition with IC_{50} value of 0.25 μ M, while the compound with allyl substitution **10d** exhibited inhibition with IC_{50} value of 0.28 μ M. Generally, the size of the linker tested ($n = 3, 5$) seems to have a small effect on the inhibitory capacity of the compounds. Overall, comparison of the AChE inhibitory activity obtained for this series of trihybrids (TAC-SAC/SPRC-BTA) with that obtained previously for the corresponding bihybrid analogues (TAC-SAC/SPRC, see Table S1 in Supplementary Data),¹⁹ showed that the inclusion of the third moiety (BTA) resulted in a considerable enhancement (up to one order of magnitude, with IC_{50} in sub- μ M range), attributable to its stronger dual-binding mode with both the CAS and PAS of AChE, especially due to the strong BTA-PAS it-it interaction.

2.3.2. Inhibition of self-mediated and Cu(II)-induced $A_{\beta 42}$ aggregation

To test the anti-amyloidogenic activity of these novel trihybrid compounds, our experimental approach relied on *in vitro* assays with thioflavine T (ThT) to monitor and quantify the aggregation of A_{342} synthetic peptide into fibrils. ThT is a histochemical dye that is known to bind to the peptide 3-sheet conformation, which is the predominant secondary structure of amyloid-beta fibrils. The presence of fibrils can be monitored by the fluorescence emission of ThT, with the absorption peak at 446 nm and the emission peak at 485 nm.^{28,29,30}

The inhibition studies were carried out upon incubating A_{342} in the presence and absence of the ligands. The results, summarized in Table 1, showed that all the compounds induced a decrease of the ThT fluorescence associated with the A3 fibril binding, thus suggesting an inhibition of the A_{342} self-aggregation process. In particular, all of them

exhibited very good-to-moderate aggregation inhibitory capacity. Compounds **10b** and **10e** showed very good inhibitory capacity (78.2% and 77.2%, respectively), while other sets of compounds (**10a**, **10c**, **10f**) and (**10d**, **10g**, **10h**) exhibited, respectively, good and moderate activities. Comparison between the anti-Af3 aggregation capacities found for these trihybrids (TAC-SAC-BTA and TAC-SPRC-BTA) and the previously reported values for corresponding bihybrids (TAC-SAC and TAC-SPRC, see Table S1)¹⁹ or tacrine itself, showed a general increase of up to 5-fold the percentage of inhibition for the same experimental conditions, which is clearly attributed to the further inclusion of the BTA moiety in these hybrids. Among the set of compounds studied herein, the chloro substitution resulted in the decrease of the interaction with Af3, with apparent slightly stronger effect for compounds with longer chain size. In general, the allylic derivatives led to a somewhat better inhibition than the corresponding propargylic ones, which may be due to higher rigidity and increased lipophilicity (some water solubility limitations).

A survey on the effect of compounds on the inhibition of copper-induced Af3 aggregation was carried out for **10c** and **10g**. It was observed a higher inhibitory activity for the incubation of Af₃₄₂ in the co-presence of copper (56.6, 37.6%) than that in its absence (31.6, 24.1%), thus suggesting that the ligands may modulate the metal-induced aggregation of Af₃₄₂, similarly to previously reported for the analogues tacrine-SAC and TAC-SPRC.²⁰ This can be rationalized by the metal-chelating properties of compounds which may compete with the amyloid peptide for the copper and decrease their aggregation ability, thus resulting in higher inhibition percentage. However, the enhancement of Af₃₄₂ inhibitory activity due to the co-presence of copper observed for the trihybrids is lower than that previously observed for dihybrids (ca 3.8 fold, see Table S1),²⁰ which may be attributed to the substitution of one N-amine by N-amide donor groups.

Insert here Table1

2.3.3. Antioxidant activity

The newly invented trihybrid compounds of TAC-SAC-BTA and TAC-SPRC-BTA were screened for their antioxidant activities, based on their interaction with the 2,2-diphenyl-1-picrylhydrazyl (DPPH) free radical.³¹ Analysis of the results evidenced low anti-

oxidant activity ($EC_{50} > 1000 \mu\text{M}$, see Fig. S10), similarly to tacrine and lower than the values previously found for the bihybrid analogues (TAC-SAC and TAC-SPRC, see Table S1),¹⁹ and so the particular values are not included herein (see representative plot in Fig. S9). These series of trihybrid compounds presented antioxidant capacity similar to tacrine, which is in contrast with the expectation due to the inclusion of the natural-based SAC and SPRC neuroprotectors.³² The recognized *in vitro* neuroprotective activity provided by these groups may be associated with an increased anti-oxidant activity inside the cells due to some enzymatic deprotection of the sulfhydryl group.³³

2.3.4. Inhibition of MAO

Four of the new compounds **10(a,c,g,h)** were investigated for their inhibitory activity against MAOs using a coupled fluorescent method.³⁴ Compounds neither quenched the fluorescence of resorufin nor compromised the activity of the coupling enzyme, horseradish peroxidase. The IC_{50} values are given in Table 1. All compounds were poor inhibitors of MAO B ($IC_{50} > 50 \mu\text{M}$), but were slightly more effective against MAO A that has a wider active site to accommodate bulky molecules.

Without preincubation, the inhibition of MAO A was less, giving IC_{50} values as follows: **10a**, 48.4 μM ; **10c**, 25.9 μM ; **10g**, 42.1 μM ; **10h**, 87.5 μM . Thus, preincubation decreased the IC_{50} only slightly (< 3-fold) in contrast to the standard MAO A inhibitor, clorgyline, where the IC_{50} decreases 100-fold with 30 min preincubation.³⁵ The very small difference in IC_{50} after 30 min preincubation was the same for both the allyl and propargyl compounds suggesting that the new propargyl derivatives do not inactivate MAO to any great extent. The high IC_{50} values obtained when inhibitor and substrate are added at the same time indicate low affinity binding, so it is likely that the propargyl group is not close enough to the N5 of the FAD in the active site of MAO to undergo enzyme-catalyzed activation.

2.3.5. Cell viability and neuroprotection

To evaluate the potential therapeutic effect of TAC-SAC-BTA and TAC-SPRC-BTA compounds **10(a–h)**, SH-SY5Y cells were treated with A₁₃₄₂ peptide or H₂O₂ in the presence or absence of the tacrine hybrids. A₁₃ peptides that accumulate in AD relevant

neurons are widely used to induce cell toxicity and model AD. Indeed, A13 oligomers induced a decrease in cell viability (Fig.4A). Despite our previous results showed that similar tacrine hybrids prevented from A13-induced cell toxicity,¹⁹ the addition of a new benzothiazol to potentiate the interaction with A13 eliminated any potential protective role. We may emphasize that an increased interaction between A13 peptides and our new tacrine hybrids 10(c,e,h) prevented A13 aggregation but still allowed soluble oligomers to interact with organelles, such as mitochondria and elicit its toxic effect. Nevertheless, compound **10d** showed the lowest inhibition of A β aggregation (14%) very similar to our data obtained with previous compounds that were able to prevent A13-induced cellular toxicity.¹⁹ Regarding compound 10f, its highest molecular weight and lipophilicity (see below and Table 1S), as well as concomitant limited solubilization, may have also contributed for the decreasing in its cellular internalization and the lowest recovering effect of the amyloid stressor..

Additionally, it is generally accepted that AD-related neurodegenerative processes involve oxidative stress that may be induced by H₂O₂.^{Indeed,} H₂O₂ (100 μ M, 24 h) induced a decrease in cell viability in SHSY-5Y cells (see Fig. 4B). Among the tacrine hybrids tested 10 (b,g,h) were the most effective in preventing H₂O₂-mediated toxicity. These results are similar to those previously obtained with other tacrine hybrid compounds.¹⁹

Insert here Fig 4

2.3.6. Pharmacokinetic properties

In an effort to establish the drug-likeness of the novel compounds and their potential to penetrate important membranes such as the blood–brain barrier (BBB), some indicators of their pharmacokinetic profiles were predicted using QikProp program, v. 2.5.³⁶ Parameters such as the calculated octanol–water partition coefficient (clogP), the ability to cross the BBB (log BB), the capacity to be absorbed through the intestinal tract to the blood (Caco-2 cell permeability), and the verification of Lipinski's rule of five, may give an idea of their drug-likeness for being orally active as anti-AD agents.

All the compounds presented clogP values greater than five (Table 1S), thus with higher lipophilic character than recommended by Lipinski's rule.³⁷ The compounds also have

molecular weights higher than 500, which accounts for two violations of this rule. The high lipophilic character and the low BBB permeability (log BB) indicate that the compounds are not eligible as drug candidates for oral administration. However, they exhibited very good results in Caco-2 permeability, ranging from ca. 600 to 1400 nm/s (higher than 500 nm/s is considered good)³⁶ with compounds 10e and 10g having lower cell permeabilities (according to the standard value). The other compounds presented greater values, indicating that the absorption through the intestinal tract to the blood is possible.

3. Conclusion

The conjugation of several functional moieties in one molecular entity has recently emerged as an important drug development strategy to combat the complex multifactorial Alzheimer's disease (AD). Following this strategy in this work, a series of eight novel trihybrids has been designed, prepared and bioassayed aimed at gathering information about potential anti-AD drug candidates. They incorporate three main moieties, tacrine (TAC), S-allyl- or S-propargyl-cysteine (SAC/SPRC) and benzothiazole (BTA), for inhibition/modulation of three main important AD targets: acetylcholinesterase inhibition, anti-oxidant activity and inhibition of amyloid 3 (A3) aggregation, with additional possible inhibition of the MAO enzyme. Analysis of the biological properties shown for these trihybrids was made in comparison with those recently reported for identical chemical library of bihybrids, lacking the BTA moiety. As hypothesized, the inclusion of the third moiety resulted in a considerable enhancement of the AChE inhibitory activity (up to one order of magnitude, with IC_{50} in sub- μ M range, below that of the tacrine drug), attributed to its stronger dual-binding mode with both the CAS and PAS of AChE, specifically due to the strong BTA-PAS it-it interaction. Also, insertion of the BTA moiety on the trihybrids led to an enhancement of up to ca 5-fold the percentage of self-A3 aggregation inhibition, attributed to the well-known affinity of BTA derivatives for A3. Nevertheless, antioxidant activity of the trihybrids is lower than the bi-hybrids and similar to that of TAC. In addition, a preliminary study with some of these new trihybrids revealed only weak capacity for MAO inhibition, another known drug target for AD.

Overall, a comparative analysis of some relevant anti-AD properties of the present trihybrids and those of the previous bihybrid analogues shows that conjugation of these three structural scaffolds in a molecular unit can provide a basis for the development of potential multifunctional drug candidates for Alzheimer's disease.

4. Experimental part

4.1. Chemistry

General methods and materials

Analytical grade reagents were purchased from Sigma-Aldrich, Fluka and Acros and were used as supplied. Solvents were dried according to standard methods³⁸. The chemical reactions were monitored by TLC using alumina plates coated with silica gel 60 F254 (Merck). Column chromatography separations were performed on silica gel Merck 230-400 mesh (Geduran Si 60). The melting points (m.p.) were measured with a Leica Galen III hot stage apparatus and are uncorrected. The ¹H and ¹³C NMR spectra were recorded on Bruker AVANCE III spectrometers at 300 and 400 MHz, respectively. Chemical shifts (δ) are reported in ppm from the standard internal reference tetramethylsilane (TMS). The following abbreviations are used: s = singlet, d = doublet, t = triplet, m = multiplet. Mass spectra (ESI-MS) were performed on a 500 MS LC Ion Trap (Varian Inc., Palo Alto, CA, USA) mass spectrometer equipped with an ESI ion source, operated in the positive ion mode. For the target compounds, the elemental analyses were performed on a Fisons EA1108 CHNS/O instrument and were within the limit of $\pm 0.4\%$. The electronic spectra were recorded with a Perkin Elmer Lambda 35 spectrophotometer, using thermostatic 1 cm path length cells.

4.1.1. General procedure for the preparation of 2-(1,2,3,4-tetrahydroacridine-9-ylamino) acid 4(a-d)

To a mixture of **3** (1 eq) and different aliphatic acids (3-aminopropanoic, 4-aminobutyric and 6-amino hexanoic acid (2 eq) was added to phenol and catalytic amount of KI. The mixture is heated at 180 °C for 4 h and then cooled to room temperature. The mixture is dissolved in 5% NaOH, washed with diethyl ether (3-4 times). The collected aqueous layer was adjusted to pH 8 with HCl, and then washed with diethyl ether (3-4 times). The aqueous layer was acidified with HCl up to pH 2 and then

extracted with dichloromethane. The organic layer was dried over anhydrous Na₂SO₄ and concentrated under reduced pressure to give the crude product. Purification was performed by column chromatography, eluent: CH₂Cl₂/MeOH (6/1) v/v, plus 10 mL 25% ammonia aqueous, for 1L total solution.

4.1.2.1. 4-(1,2,3,4-tetrahydroacridin-9-ylamino)butanoic acid (4a)

9-Chloro-1,2,3,4-tetrahydroacridine (3a) and 4-aminobutyric acid afforded the pure title product as a light yellow colour solid; yield 62%; m.p. 157-160 °C; ¹H NMR (MeOD) δ: 8.45 (d, *J* = 8.6 Hz, 1H, H-8), 7.85-7.73 (m, 2H, H-5 & H-6), 7.59-7.53 (m, 1H, H-7), 4.00 (t, *J* = 7.0 Hz, 2H, H-1'), 3.00 (brs, 2H, H-4), 2.69 (brs, 2H, H-1), 2.50 (t, *J* = 6.7 Hz, 2H, H-3'), 2.16-2.07 (m, 2H, H-2'), 1.96-1.93 (m, 4H, H-2 & H-3); MS-ESI (*m/z*): 285 (M+1)⁺, 286 (M+2)⁺.

4.1.2.2. 6-(1,2,3,4-tetrahydroacridin-9-ylamino)hexanoic acid (4b)

9-Chloro-1,2,3,4-tetrahydroacridine (3a) and 6-aminohexanoic acid afforded the pure title product as a light yellow colour solid; yield 67%; m.p. 181-183 °C; ¹H NMR (300 MHz, MeOD) δ: 8.19 (d, *J* = 8.5 Hz, 1H, H-8), 8.04 (d, *J* = 8.4 Hz, 1H, H-5), 7.68-7.62 (m, 1H, H-6), 7.44-7.39 (m, 1H, H-7), 3.85 (t, *J* = 7.0 Hz, 2H, H-1'), 3.00 (brs, 2H, H-4), 2.59 (brs, 2H, H-1), 2.24 (t, *J* = 7.0 Hz, 2H, H-5'), 1.85-1.79 (m, 6H, H-2, H-3, & H-2'), 1.61-1.59 (m, 2H, H-4'), 1.42-1.39 (m, 2H, H-3'); MS-ESI (*m/z*): 313 (M+1)⁺, 314 (M+2)⁺.

4.1.2.3. 4-(6-chloro-1,2,3,4-tetrahydroacridin-9-ylamino)butanoic acid (4c)

6,9-Chloro-1,2,3,4-tetrahydroacridine (3b) and 4-aminobutyric acid afforded the pure title product as a light yellow colour solid; yield 59%; m.p. 230-232 °C; ¹H NMR (MeOD) δ: 8.45 (d, *J* = 8.7 Hz, 1H, H-8), 7.76 (d, *J* = 1.9 Hz, 1H, H-5), 7.52 (dd, *J* = 7.2 & 1.9 Hz, 1H, H-7), 4.00 (t, *J* = 6.9 Hz, 2H, H-1'), 3.00 (brs, 2H, H-4), 2.71 (brs, 2H, H-1), 2.50 (t, *J* = 8.1 Hz, 2H, H-3'), 2.20-2.13 (m, 2H, H-2'), 1.99-1.96 (m, 4H, H-2 & H-3); MS-ESI (*m/z*): 318 (M)⁺, 319 (M+1)⁺.

4.1.2.4. 6-(6-chloro-1,2,3,4-tetrahydroacridin-9-ylamino)hexanoic acid (4d)

6,9-Chloro-1,2,3,4-tetrahydroacridine (3b) and 6-aminohexanoic acid afforded the pure title product as a light yellow colour solid; yield 69%; m.p. 155-157 °C; ¹H NMR

(300 MHz, MeOD) δ 8.39 (d, $J = 8.9$ Hz, H-8), 7.82 (d, $J = 2.1$ Hz, 1H, H-5), 7.55 (dd, 1H, $J = 7.0$ & 2.1 Hz, H-7), 3.98 (t, $J = 7.2$ Hz, 2H, H-1'), 3.00 (br, 2H, H-4), 2.72 (br, 2H, H-3), 2.35 (t, $J = 7.2$ Hz, 2H, H-5'), 2.00-1.98 (m, 4H, H-2 & H-3); 1.94-1.86 (m, 2H, H-2'), 1.73-1.65 (m, 2H, H-4'), 1.55-1.49 (m, 2H, H-3'); MS-ESI (m/z): 346 (M^+), 347 ($M+1$)⁺.

4.1.4. Procedure for the preparation of 3-allylsulfanyl-2-amino-propionic acid (6a) and 2-amino-3-prop-ynylsulfanyl-propionic acid (6b)

L-cysteine (1 eq) were dissolved in NH_4OH solution (2M, 45 mL), and the reaction mixture was stirred at 0 °C around 30 min. Afterwards, allyl bromide/propargyl bromide (1.5 eq) was dropwise added and reaction mixture was stirred for another 3 h, concentrated *in vacuo* and filtered; the filtrate was washed with ethanol and recrystallized from water-ethanol affording the pure product as white shiny particles.

4.1.3.1. (R)-3-allylsulfanyl-2-amino-propionic acid (6a)

L-cysteine (5) and allyl bromide afforded the pure title product as a white powder; yield 75%; m.p. 220-221 °C; ^1H NMR (300 MHz, D_2O) δ : 5.96-5.79 (m, 1H, $\text{HC}=\text{C}$), 5.29-5.19 (m, 2H, $\text{CH}_2=\text{CH}$), 3.94-3.82 (m, 1H, CHNH_2), 3.21 (d, $J = 7.2$ Hz, 2H, CH_2 -allyl), 3.00-2.94 (m, 2H, CH_2CHN); MS-ESI (m/z): 160($M-1$)⁺, 162($M+1$)⁺.

4.1.3.2. (R)-2-amino-3-prop-ynylsulfanyl-propionic acid (6b)

L-cysteine (5) and propargyl bromide afforded the pure title product as a white shiny solids; yield 72%; m.p. 294-296 °C; ^1H NMR (300 MHz, D_2O) δ : 3.83-3.90 (m, 1H, CHNH_2), 3.32-3.30 (m, 2H, CH_2 -propargyl), 3.24-3.01 (m, 2H, CH_2CHN), 2.61 (t, $J = 2.5$ Hz, 1H, HCC); MS-ESI (m/z): 160 ($M+1$)⁺.

4.1.4. Procedure for the preparation of (S)-3-(allylthio)-2-(tert-butoxycarbonylamino)propionic acid (7a) and (S)-2-(tert-butoxycarbonylamino)-3-(prop-2-ynylthio)propanoic acid (7b)

Compound 6(a, b) (1 eq) and *Boc* anhydride (1 eq) were both dissolved and stirred in THF (25 mL), saturated with sodium bicarbonate solution (60 mL) and left stirring for 5 h at room temperature. The reaction mixture was diluted with H_2O (15 mL) and EtOAc (15 mL), the pH was adjusted to about 2-2.5, and then separate the organic

extracts were washed with brine and dried over Na₂SO₄. The solvent was removed under vacuum and the crude material was purified by silica gel chromatography to give **7(a,b)**.

4.1.4.1. (S)-3-(allylthio)-2-(tert-butoxycarbonylamino)propanoic acid (**7a**)

3-Allylsulfanyl-2-amino-propionic acid (**6a**) was treated with *Boc* anhydride to afford the pure title product as semi solid; yield 90%; ¹H NMR (300 MHz, DMSO-*d*₆) 5: 7.1 (d, *J* = 8.3 Hz, 1H, *HNCH*), 5.79-5.69 (m, 1H, *HC=C*), 5.14-5.06 (m, 2H, *CH₂=HC*), 4.06-4.01(m, 1H, *CHNH*), 3.15 (d, *J* = 7.1 Hz, 2H, *CH₂-allyl*), 2.82-2.61 (m, 2H, *CH₂CHN*), 1.38 (s, 9H, *tBuH*); MS-ESI (*m/z*): 261 (M⁺).

4.1.4.2. (S)-2-(tert-butoxycarbonylamino)-3-(prop-2-ynylthio)propanoic acid (**7b**)

2-Amino-3-prop-ynylsulfanyl-propionic acid (**6b**) and *Boc* anhydride afforded the pure title product as semi solid; yield 83%; ¹H NMR (300 MHz, DMSO) 5: 7.15 (d, *J* = 8.4 Hz, 1H, *HNCH*), 4.15-4.08 (1H, m, *HCNH*), 3.41-3.39 (m, 2H, *CH₂-propargyl*), 3.08-3.81 (m, 2H, *CH₂CHN*), 2.67 (t, *J* = 2.5 Hz, 1H, *HCC*), 1.41 (s, 9H, *tBuH*); MS-ESI (*m/z*): 259 (M⁺).

4.1.5. Procedure for the preparation of tert-butyl 3-(allylthio)-1-(benzo[d]thiazol-2-ylamino)-1-oxopropan-2-yl-carbamate (**8a**) and tert-butyl 1-(benzo[d]thiazol-2-ylamino)-1-oxo-3-(prop-2-ynylthio)propan-2-yl-carbamate (**8b**)

T₃P (1.5 eq) was added dropwise to a stirred suspension of 2-amino benzothiazole (1 eq) (**8**), *N*-Boc protected SAC/SPRC (1 eq) **7(a,b)** and NMM (2.5 eq) in DCM under nitrogen and the mixture was stirred at room temperature for 3 h; after completing the reaction, it was diluted with water and extracted in ethyl acetate (3×20 mL). The combined extracts were washed with HCl (0.1 N, 3×50 mL) and NaOH (1 N, 3×50 mL) and then with water and brine. The combined organic phases were dried over Na₂SO₄ and solvent was removed to afford the substituted compounds **8(a,b)**.

4.1.5.1. Tert-butyl-3-(allylthio)-1-(benzo[d]thiazol-2-ylamino)-1-oxopropan-2-yl-carbamate (**8a**)

2-Aminobenzothiazole (**8**) and *N*-Boc protected SAC (**7a**) afforded the pure title product as an colorless solid with 78% yield; m.p. 83-85 °C; ¹H NMR (300 MHz, CDCl₃) 5: 7.82-7.83 (m, 2H, H-4 & H-7), 7.43 (t, *J* = 8.0 Hz, 1H, H-5 or H-6), 7.31 (t, *J* = 8.0 Hz, 1H, H-6 or H-5), 5.73-5.65 (m, 1H, *HC=C*), 5.11-5.07 (m, 2H, *H₂C=CH*), 4.66-4.55 (m,

1H, HCNH), 3.08 (d, $J = 7.1$ Hz, 2H, CH₂-allyl), 2.98-2.95 (m, 2H, CH₂CHN), 1.46 (s, 9H, *t*BuH); MS-ESI (m/z): 393 (M⁺).

4.1.5.2. Tert-butyl-1-(benzo[d]thiazol-2-ylamino)-1-oxo-3-(prop-2-ynylthio)propan-2-yl-carbamate (8b)

2-Aminobenzothiazole (**8**) and *N*-Boc protected SPRC (**7b**) afforded the pure title product as a colourless solid; yield 83%; m.p.133-135 °C; ¹H NMR (300 MHz, CDCl₃) 5: 7.82-7.85 (m, 2H, H-4 & H-7), 7.45 (t, $J = 8.0$ Hz, 1H, H-5 or H-6), 7.31 (t, $J = 8.0$ Hz, 1H, H-6 or H-5), 4.82-4.80 (1H, m, HCNH), 3.26-3.22 (m, 4H, CH₂-propargyl, & CH₂CHN), 2.26 (s, 1H, HCC), 1.41 (s, 9H, *t*BuH); MS-ESI (m/z): 391 (M⁺).

4.1.6. Procedure for the preparation of 3-(allylthio)-2-amino-N-(benzo[d]thiazol-2-yl)propanamide (9a) and 2-amino-N-(benzo[d]thiazol-2-yl)-3-(prop-2-ynylthio)propanamide (9b)

Compounds **8(a,b)** and trifluoroacetic acid (TFA, 1 mL) were dissolved DCM (2 mL) and stirred at room temperature for 2 h. After completing the reaction, the solvent was evaporated and afforded the crude product and washed with diluted ammonia solution (10%). Purification was performed by column chromatography, eluent CH₂Cl₂/MeOH (6/1), affording pure compounds **9(a,b)**.

4.1.6.1. 3-(allylthio)-2-amino-N-(benzo[d]thiazol-2-yl)propanamide (9a)

Tert-butyl-3-(allylthio)-1-(benzo[d]thiazol-2-ylamino)-1-oxopropan-2-yl-carbamate (**8a**) and TFA afforded the pure title product as a colourless solid; yield 86%; m.p.105-107 °C; ¹H NMR (CDCl₃) 5: 7.78-7.82 (m, 2H, H-4 & H-7), 7.44 (t, $J = 8.0$ Hz, 1H, H-5 or H-6), 7.29 (t, $J = 8.0$ Hz, 1H, H-6 or H-5), 5.71-5.22 (m, 1H, HC=C), 5.135.20 (m, 2H, H₂C=CH), 3.79 (brs, 1H, HCNH), 3.08-3.15 (m, 3H, H₂C-allyl & H₂CCHN), 3.09-2.80 (m, 1H, H₂CCHN); MS-ESI (m/z): 293 (M⁺).

4.1.6.2. 2-amino-N-(benzo[d]thiazol-2-yl)-3-(prop-2-ynylthio)propanamide (9b)

Tert-butyl-1-(benzo[d]thiazol-2-ylamino)-1-oxo-3-(prop-2-ynylthio)propan-2-yl-carbamate (**8b**) and TFA afforded the pure title product as a colourless solid; yield 89%; m.p.112-114 °C; ¹H NMR (DMSO) 5: 7.98 (d, $J = 7.8$ Hz, 1H, H-4) 7.75 (d, $J = 7.8$ Hz, 1H, H-7), 7.45 (t, $J = 8.0$ Hz, 1H, H-5 or H-6), 7.32 (t, 1H, $J = 8.0$ Hz, H-6 or H-5), 3.76

(t, J = 6.7 Hz, 1H, HCNH), 3.19 (s, J = 6.7 Hz, 2H, CH₂-propargyl), 2.97-2.86 (m, 3H, -CH₂CHN & HCC); MS-ESI (m/z): 291 (M⁺).

4.1.7. General procedure for the preparation of 10(a-h)

T₃P (1.5 eq) was added dropwise to a stirred suspension of BTA-SAC/BTA-SPRC (1 eq) **9(a,b)**, 2-(1,2,3,4-tetrahydroacridine-9-ylamino) acid (1 eq) **4(a-d)** and NMM (2.5 eq) in DCM under nitrogen and the mixture was stirred at room temperature for 3 h; after completing the reaction, it was diluted with water and extracted in ethyl acetate (3x20 mL). The combined extracts were washed with HCl (0.1N, 3x50 mL) and NaOH (1N, 3x50 mL) and then with water and brine. The combined organic phases were dried over Na₂SO₄ and solvent was removed to afford the substituted compounds **10(a-h)**. The final product was purified by column chromatography, eluent: CH₂Cl₂/MeOH (6/1) v/v, plus 10 mL 25% ammonia aqueous, for 1L total solution and some of the compounds recrystallized by ethanol and ethyl ether.

4.1.7.1. N-(3-(Allylthio)-1-(benzo[d]thiazol-2-ylamino)-1-oxopropan-2-yl)-4-(1,2,3,4-tetrahydroacridin-9-ylamino)butanamide (10a)

3-(Allylthio)-2-amino-N-(benzo[d]thiazol-2-yl)propanamide (**9a**) and 4-(1,2,3,4-tetrahydroacridin-9-ylamino)butanoic acid (**4a**) afforded the pure title product as a light yellow color solid; yield 65%; m.p. 95-102 °C; ¹H NMR (400 MHz, MeOD-d₄) δ: 8.33-8.34 (m, 1H, H-8), 7.75-7.78 (m, 2H, H-4''' & H-7'''), 7.60-7.64 (m, 2H, H-5 & H-6), 7.47-7.52 (m, 1H, H-5''' or H-6'''), 7.40-7.41 (m, 1H, H-6''' or H-5'''), 7.29-7.30 (m, 1H, H-7), 5.70-5.80 (m, 1H, CH-allyl), 5.14 (d, 1H, J = 16.0 Hz, CH₂-allyl), 5.08 (d, 1H, J = 8.0 Hz, CH₂-allyl), 4.72 (t, J = 8.0 Hz, 1H, H-2''), 3.88-3.90 (m, 2H, H-1'), 3.11-3.18 (m, 3H, -SCH₂-allyl & H-3''), 2.94-2.2.99 (m, 3H, H-4 & H-3''), 2.74 (brs, 2H, H-1), 2.55 (t, J = 8.0 Hz, 2H, H-3'), 2.10-2.15 (m, 2H, H-2'), 1.85 (brs, 4H, H-2 & H-3); ¹³C NMR (100.5 MHz, DMSO-d₆) δ: 172.8, 171.0, 158.1, 157.3, 151.6, 148.9, 145.9, 134.6, 131.9, 129.0, 126.6, 124.1, 123.9, 123.8, 122.2, 121.0, 120.0, 117.9, 115.7, 53.0, 47.9, 34.4, 34.2, 33.1, 32.8, 31.9, 31.7, 26.8, 25.3, 22.9, 22.5; MS-ESI (m/z): 558 (M-1)⁺, 559 (M⁺), 560 (M+1)⁺; Analysis calc. for C₃₀H₃₃N₅O₂S₂·0.52 EtOH: C 62.83, H 6.06, N 12.01, S 11.00 %; found: C 63.05, H 6.21, N 11.61 %.

4.1.7.2. **N-(3-(Allylthio)-1-(benzo[d]thiazol-2-ylamino)-1-oxopropan-2-yl)-6-(1,2,3,4-tetrahydroacridin-9-ylamino)hexanamide (10b)**

3-(Allylthio)-2-amino-N-(benzo[d]thiazol-2-yl)propanamide (**9a**) and 6-(1,2,3,4-tetrahydroacridin-9-ylamino)hexanoic acid (**4b**) afforded the pure title product as a light yellow color solid; yield 71 %; m.p. 96-100 °C ; ¹H NMR (400 MHz, MeOD-d₄) δ: 8.13 (d, J = 8.0 Hz, 1H, H-8), 7.67-7.75(m, 2H, H-4''' & H-7'''), 7.59 (t, J = 8.0 Hz, 1H, H-5), 7.39 (t, J = 8.0 Hz, 1H, H-6), 7.36-7.37 (m, 2H, H-5''' & H-6'''), 7.25 (t, J = 8.0 Hz, 1H, H-7), 5.50-5.78 (m, 1H, CH-allyl), 5.13 (d, 1H, J = 20.0 Hz, =CH₂-allyl), 5.06 (d, 1H, J = 8.0 Hz, =CH₂-allyl), 4.75 (t, 1H, J = 8.0 Hz, H-2''), 3.61 (t, 2H, J = 8.0 Hz, H-1'), 3.15 (d, 2H, J = 8.0 Hz, CH₂-allyl), 2.93-2.96 (m, 3H, H-4 & H-3''), 2.86-2.88 (m, 1H, H-3''), 2.68 (brs, 2H, H-1), 2.30 (t, J = 8.0 Hz, 2H, H-5'), 1.87 (brs, 4H, H-2 & H-3), 1.66-1.73 (m, 4H, H-2' & H-4'), 1.42-1.45 (m, 2H, H-3'); ¹³C NMR (100.5 MHz, MeOD-d₄) δ: 174.7, 170.9, 159.1, 155.5, 153.1, 148.4, 144.1, 133.9, 131.9, 129.5, 125.8, 124.3, 123.7, 123.6, 123.4, 120.8, 120.2, 116.6, 53.1, 51.8, 35.0, 34.2, 31.6, 31.4, 30.3, 29.3, 25.9, 24.9, 24.3, 22.4, 21.7; MS-ESI (m/z): 588(M⁺), 589 (M+1)⁺, 590 (M+2)⁺; Analysis calc. for C₃₂H₃₇N₅O₂S₂.0.20 EtOH.0.5 H₂O: C 63.42, H 6.65, N 11.56%; found: C 63.01, H 6.62, N 11.37%.

4.1.7.3. **N-(3-(Allylthio)-1-(benzo[d]thiazol-2-ylamino)-1-oxopropan-2-yl)-4-(6-chloro-1,2,3,4-tetrahydroacridin-9-ylamino)butanamide (10c)**

3-(Allylthio)-2-amino-N-(benzo[d]thiazol-2-yl)propanamide (**9a**) and 4-(6-chloro-1,2,3,4-tetrahydroacridin-9-ylamino)butanoic acid (**4c**) afforded the pure title product as a light yellow color solid; yield 61%; m.p. 195-198 °C; ¹H NMR (400 MHz, MeOD-d₄) δ: 8.15 (d, J = 8.0 Hz, 1H, H-8), 7.80 (d, J = 8.0 Hz, 1H, H-5) 7.62-7.67 (m, 2H, H-4''' & H-7'''), 7.40 (t, J = 8.0 Hz, 1H, H-7), 7.27-7.33 (m, 2H, H-5''' & H-6'''), 5.70-5.80 (m, 1H, CH-allyl), 5.13 (d, 1H, J = 20.0 Hz, CH₂-allyl), 5.07 (d, 1H, J = 8.0 Hz, CH₂-allyl), 4.73 (t, J = 8.0 Hz, 1H, H-2''), 3.68 (t, 2H, J = 8.0 Hz, H-1'), 3.14 (d, 2H, J = 8.0 Hz, -SCH₂-allyl), 2.91-2.94 (m, 1H, H-3''), 2.83-2.86 (m, 3H, H-4 & H-3''), 2.67 (brs, 2H, H-1), 2.47 (t, J = 8.0 Hz, 2H, H-3'), 2.05-2.06 (m, 2H, H-2'), 1.84 (brs, 4H, H-2 & H-3); ¹³C NMR (100.5 MHz, DMSO-d₆) δ: 172.8, 171.0, 158.6, 158.0, 151.6, 148.9, 147.6, 134.6, 133.5, 131.9, 126.7, 126.3, 124.2 124.1, 122.2 121.0, 117.9, 115.9, 53.0, 47.9, 34.2, 33.2, 32.8, 31.9, 26.8, 25.3, 22.8, 22.4; MS-ESI (m/z): 594 (M⁺), 595 (M+1)⁺, 596

(M+2)⁺; Analysis calc. for C₃₀H₃₂N₅O₂S₂Cl. 0.70 H₂O: C 59.38, H 5.55, N 11.54 %; found : C 59.07, H 5.55, N 11.36 %.

4.1.7.4. N-(3-(Allylthio)-1-(benzo[d]thiazol-2-ylamino)-1-oxopropan-2-yl)-6-(6-chloro-1,2,3,4-tetrahydroacridin-9-ylamino)hexanamide (10d)

3-(Allylthio)-2-amino-*N*-(benzo[d]thiazol-2-yl)propanamide (**9a**) and 6-(6-chloro-1,2,3,4-tetrahydroacridin-9-ylamino)hexanoic acid (**4d**) afforded the pure title product as a light yellow color solid; yield 68 %; m.p. 94-98 °C; ¹H NMR (400 MHz, MeOD-*d*₄) δ: 8.11 (d, *J* = 8.0 Hz, 1H, H-8), 7.76 (d, *J* = 8.0 Hz, 1H, H-4''') 7.69-7.71 (m, 2H, H-5 & H-7'''), 7.40 (t, *J* = 8.0 Hz, 1H, H-5''' or H-6'''), 7.32-7.35 (m, 1H, H-7), 7.27 (t, *J* = 8.0 Hz, 1H, H-6''' or H-5'''), 5.72-5.79 (m, 1H, CH-allyl), 5.14 (d, 1H, *J* = 20.0 Hz, =CH₂-allyl), 5.08 (d, 1H, *J* = 12.0 Hz, =CH₂-allyl), 4.75 (t, *J* = 8.0 Hz, 1H, H-2''), 3.59 (t, 2H, *J* = 8.0 Hz, H-1'), 3.15 (d, 1H, *J* = 4.0 Hz, CH₂-allyl), 2.92-2.98 (m, 3H, H-4 & H-3''), 2.80-2.83 (m, 1H, H-3''), 2.67 (brs, 2H, H-1), 2.30 (t, *J* = 8.0 Hz, 2H, H-3'), 1.88 (brs, 4H, H-2 & H-3), 1.66-1.73 (m, 4H, H-2' & H-4'), 1.40-1.48 (m, 2H, H-3'); ¹³C NMR (100.5 MHz, DMSO-*d*₆) δ: 172.9, 171.2, 159.7, 158.3, 150.9, 148.9, 148.0, 134.6, 132.9, 131.9, 127.1, 126.5, 125.9, 123.8, 121.0, 119.0, 117.9, 116.3, 53.0, 48.3, 35.3, 34.2, 33.9, 32.0, 30.7, 26.3, 25.4, 25.3, 23.0, 22.7; MS-ESI (*m/z*): 622 (M⁺), 623 (M+1)⁺, 624 (M+2)⁺; Analysis calc. for C₃₂H₃₆N₅O₂S₂Cl.0.79 EtOH: C 61.24, H 6.23, N 10.63 %; found: C 61.08, H 6.38, N 10.30 %.

4.1.7.5. N-(1-(Benzo[d]thiazol-2-ylamino)-1-oxo-3-(prop-2-ynylthio)propan-2-yl)-4-(1,2,3,4-tetrahydroacridin-9-ylamino)butanamide (10e)

2-Amino-*N*-(benzo[d]thiazol-2-yl)-3-(prop-2-ynylthio)propanamide (**9b**) and 4-(1,2,3,4-tetrahydroacridin-9-ylamino)butanoic acid (**4a**) afforded the pure title product as a light yellow color solid; yield 63%; m.p. 105-110 °C; ¹H NMR (400 MHz, MeOD-*d*₄) δ: 8.17 (d, *J* = 8.0 Hz, 1H, H-8), 7.78 (d, *J* = 8.0 Hz, H-4''') 7.64-7.70 (m, 2H, H-5 & H-7'''), 7.56 (t, *J* = 8.0 Hz, 1H, H-6), 7.39 (t, 2H, *J* = 8.0 Hz, H-5''' & H-6'''), 7.27 (t, *J* = 8.0 Hz, 1H, H-7), 4.82 (t, 1H, *J* = 8.0 Hz, H-2''), 3.69 (t, 2H, *J* = 8.0 Hz, H-1'), 3.35 (s, 2H, -SCH₂-propargyl), 3.21-3.26 (m, 1H, H-3''), 3.01-3.06 (m, 1H, H-3''), 2.90 (brs, 2H, H-4), 2.72 (brs, 2H, H-1), 2.60 (s, 1H, -CH-propargyl), 2.48 (t, *J* = 8.0 Hz, 2H, H-3'), 2.04-2.09 (m, 2H, H-3'), 1.86 (brs, 4H, H-2 & H-3); ¹³C NMR (100.5 MHz, DMSO-*d*₆) δ: 172.8,

171.0, 158.2, 157.7, 151.1, 148.9, 146.6, 131.9, 128.6, 127.7, 126.6, 124.1, 123.8, 123.6, 122.19, 121.0, 120.3, 116.1, 80.6, 74.4, 52.8, 48.0, 33.4, 32.8, 26.9, 25.4, 23.1, 22.7, 19.1; MS-ESI (m/z): 556(M-1)⁺, 557(M⁺), 558 (M+1)⁺; Analysis calc. for C₃₀H₃₁N₅O₂S₂·0.23 EtOH: C 63.00, H 5.66, N 12.32, S 11.28%; found: C 64.02, H 5.79, N 12.18%.

4.1.7.6. N-(1-(Benzo[d]thiazol-2-ylamino)-1-oxo-3-(prop-2-ynylthio)propan-2-yl)-6-(1,2,3,4-tetrahydroacridin-9-ylamino)hexanamide (10f)

2-Amino-*N*-(benzo[d]thiazol-2-yl)-3-(prop-2-ynylthio)propanamide (**9b**) and 6-(1,2,3,4-tetrahydroacridin-9-ylamino)hexanoic acid (**4b**) afforded the pure title product as a light yellow color solid; yield 75%; m.p. 96-100 °C; ¹H NMR (400 MHz, MeOD-*d*₄) δ: 8.30 (d, J = 8.0 Hz, 1H, H-8), 7.78 (m, 2H, H-4''' & H-7'''), 7.50-7.54 (m, 1H, H-5), 7.39 (t, 2H, J = 8.0 Hz, H-6), 7.26 (t, J = 8.0 Hz, 1H, H-5''' or H-6'''), 7.15 (t, J = 8.0 Hz, 1H, H-6''' or H-5'''), 6.75-6.80 (m, 1H, H-7), 4.82 (t, 1H, J = 8.0 Hz, H-2''), 3.86 (t, 2H, J = 8.0 Hz, H-1'), 3.37 (s, 2H, -SCH₂-propargyl), 3.18-3.23 (m, 1H, H-3''), 3.01-3.07 (m, 1H, H-3''), 2.93 (brs, 2H, H-4), 2.63-2.64 (m, 3H, H-1 & -CH-propargyl), 2.35 (t, J = 8.0 Hz, 2H, H-5'), 1.91 (brs, 4H, H-2 & H-3), 1.79-1.87 (m, 2H, H-2'), 1.69-1.73 (m, 2H, H-4'), 1.48-1.53 (m, 2H, H-3'); ¹³C NMR (100.5 MHz, DMSO-*d*₆) δ: 173.0, 171.1, 158.3, 158.0, 151.0, 148.9, 146.9, 131.9, 128.5, 128.3, 126.6, 124.0, 123.7, 123.6, 122.1, 121.0, 120.4, 116.0, 80.6, 74.3, 52.8, 48.3, 35.3, 33.7, 32.9, 30.8, 26.3, 25.4, 25.3, 23.1, 22.8, 19.1; MS-ESI (m/z): 584(M-1)⁺, 585(M⁺), 586 (M+1)⁺; Analysis calc. for C₃₀H₃₁N₅O₂S₂·0.51 EtOH: C 64.06, H 6.13, N 11.49, S 10.52%; found: C 64.01, H 5.85, N 11.20%.

4.1.7.7. N-(1-(Benzo[d]thiazol-2-ylamino)-1-oxo-3-(prop-2-ynylthio)propan-2-yl)-4-(6-chloro-1,2,3,4-tetrahydroacridin-9-ylamino)butanamide (10g)

2-Amino-*N*-(benzo[d]thiazol-2-yl)-3-(prop-2-ynylthio)propanamide (**9b**) and 4-(6-chloro-1,2,3,4-tetrahydroacridin-9-ylamino)butanoic acid (**4c**) afforded the pure title product as a light yellow color solid; yield 63%; m.p. 119-122 °C; ¹H NMR (400 MHz, MeOD-*d*₄) δ: 8.19 (d, J = 8.0 Hz, 1H, H-8), 7.80 (d, J = 8.0 Hz, 1H, H-4'''), 7.61-7.65 (m, 2H, H-5 & H-7'''), 7.41 (t, J = 8.0 Hz, 1H, H-5''' or H-6'''), 7.35 (d, 1H, J = 8.0 Hz, H-7), 7.30 (t, J = 8.0 Hz, 1H, H-6''' or H-5'''), 4.80 (t, 1H, J = 8.0 Hz, H-2''), 3.73 (t, 2H, J = 8.0 Hz, H-1'), 3.36 (s, 2H, -SCH₂-propargyl), 3.18-3.23 (m, 1H, H-3''), 3.03-3.07 (m,

1H, H-3''), 2.84-2.86 (m, 2H, H-4), 2.67 (brs, 2H, H-1), 2.62 (s, 1H, -CH-propargyl), 2.49 (t, $J = 8.0$ Hz, 2H, H-3'), 2.07-2.10 (m, 2H, H-3'), 1.85 (brs, 4H, H-2 & H-3); ^{13}C NMR (100.5 MHz, MeOD- d_4) δ : 174.4, 170.3, 158.1, 155.7, 153.4, 148.3, 144.1, 135.7, 131.9, 126.0, 125.8, 124.3, 123.6, 122.3, 120.8, 120.3, 116.6, 114.2, 78.9, 71.6, 53.0, 49.3, 32.6, 32.1, 30.9, 29.2, 25.8, 24.1, 22.1, 18.5; MS-ESI (m/z): 592 (M^+), 593($\text{M}+1$) $^+$, 594 ($\text{M}+2$) $^+$; Analysis calc. for $\text{C}_{30}\text{H}_{30}\text{N}_5\text{O}_2\text{S}_2\text{Cl} \cdot 0.98\text{H}_2\text{O} \cdot 0.9\text{EtOH}$: C 58.64, H 5.78, N 10.75%; found: C 58.06, H 5.34, N 11.07%.

4.1.7.8. N-(1-(Benzo[d]thiazol-2-ylamino)-1-oxo-3-(prop-2-ynylthio)propan-2-yl)-6-(6-chloro-1,2,3,4-tetrahydroacridin-9-ylamino)hexanamide (10h)

2-Amino-*N*-(benzo[d]thiazol-2-yl)-3-(prop-2-ynylthio)propanamide (**9b**) and 6-(6-chloro-1,2,3,4-tetrahydroacridin-9-ylamino)hexanoic acid (**4d**) afforded the pure title product as a light yellow color solid; yield 70%; m.p. 98-106 °C; ^1H NMR (400 MHz, MeOD- d_4) δ : 8.10 (d, $J = 8.0$ Hz, 1H, H-8), 7.75 (d, $J = 8.0$ Hz, 1H, H-4'''), 7.68-7.70 (m, 2H, H-5 & H-7'''), 7.39 (t, $J = 8.0$ Hz, 1H, H-5''' or H-6'''), 7.33 (d, 1H, $J = 8.0$ Hz, H-7), 7.27 (t, $J = 8.0$ Hz, 1H, H-6''' or H-5'''), 4.83 (t, 1H, $J = 8.0$ Hz, H-2''), 3.59 (t, 2H, $J = 8.0$ Hz, H-1'), 3.36 (s, 2H, -SCH₂-propargyl), 3.18-3.23 (m, 1H, H-3''), 3.03-3.06 (m, 1H, H-3''), 2.92 (brs, 2H, H-4), 2.66 (brs, 2H, H-1), 2.62 (m, 1H, -CH-propargyl), 2.32 (t, $J = 8.0$ Hz, 2H, H-5'), 1.88 (brs, 4H, H-2 & H-3), 1.67-1.73 (m, 4H, H-2' & H-4'), 1.42-1.48 (m, 2H, H-3'); ^{13}C NMR (100.5 MHz, DMSO- d_6) δ : 173.0, 170.9, 158.2, 158.0, 151.8, 148.8, 146.4, 133.7, 131.9, 126.6, 126.3, 125.5, 124.1, 122.1, 121.0, 118.2, 115.5, 80.6, 74.3, 52.8, 48.1, 35.2, 32.9, 30.6, 26.3, 25.3, 25.2, 22.8, 22.3, 19.1; MS-ESI (m/z): 620 (M^+), 620 ($\text{M}+1$) $^+$, 621 ($\text{M}+2$) $^+$; Analysis calc. for $\text{C}_{32}\text{H}_{34}\text{N}_5\text{O}_2\text{S}_2\text{Cl} \cdot 1.1 \text{EtOH}$: C 61.23, H 6.10, N 10.44%; found: C 61.57, H 6.15, N 9.87%.

4.2. Molecular Modeling

To perform our docking studies the X-ray crystallographic structure of *Torpedo californica*-AChE (*Tc*AChE) complexed with an inhibitor was taken from RCSB Protein Data Bank (PDB entry 1ODC), in order to be used as receptor. This structure was chosen because of the similarity between its original inhibitor ((*N*-4'-quinolyl-*N'*-9''-(1'',2'',3'',4''-tetrahydroacridinyl)-1,8-diaminooctane) and our ligands: all have a tacrine moiety and an aromatic group linked through an alkyl chain.³⁹ The original structure was treated using

Maestro v. 9.3⁴⁰ by removing the original ligand, solvent, and cocrystallization molecules, and then adding the hydrogen atoms. The ligands were built using Maestro, and then, using Ghemical v. 2.0⁴¹ they were submitted to random conformational search (RCS) of 1000 cycles, and 2500 optimization steps using Tripos 5.2 force field.⁴² The minimized ligands were docked into the AChE structure with GOLD software v. 5.1,⁴³ and the zone of interest was defined as the residues within 10 Å from the original position of the ligand in the crystal structure. The ‘allow early termination’ option was deactivated, and the remaining default parameters of Gold were used. The ligands were subjected to 100 genetic algorithm steps using ASP as fitness function.

4.3. Prediction of pharmacokinetic properties

To analyze the potential of the new compounds as new anti-AD drugs, a brief prediction on pharmacokinetic proprieties was performed *in silico*. Parameters such as the lipophilic character (clogP), blood–brain barrier partition coefficient (log BB), the ability to be absorbed through the intestinal tract (Caco-2 cell permeability) and CNS activity were calculated.

The ligands were built and minimized as previously mentioned for the docking studies. The structures were submitted to the calculation of these relevant pharmacokinetic proprieties and descriptors using QikProp v. 2.5.³⁶ These predictions are for orally delivered drugs and assume nonactive transport

4.4. Antioxidant activity:

The antioxidant activity was evaluated by the DPPH method previously described.³¹ To a 2.5-mL solution of DPPH (0.002%) in methanol, four samples of each compound in solution were added in different volumes to obtain different concentrations in a 3.5-mL final volume. The samples were incubated for 30 min at room temperature.

The absorbance was measured at 517 nm against the corresponding blank (methanol). The antioxidant activity was calculated by an Eq. (3).⁴⁴

$$\%AA = \frac{A_{DPPH} - A_{sample}}{A_{DPPH}} \quad (3)$$

The tests were carried out in triplicate. The compound concentrations providing 50% of antioxidant activity (EC_{50}) were obtained by plotting the antioxidant activity against the compound concentration.

4.5. Acetylcholinesterase activity

The enzymatic activity *TcACHE* was measured using an adaptation of the method previously described.¹⁵ The assay solution contained 374 μ L of HEPES buffer (50 mM and pH 8.0), a variable volume (10–50 μ L) of the stock solution of each compound in methanol (1 mg/mL), 25 μ L of AChE stock solution, and the necessary amount of methanol to attain 0.925 mL of the sample mixture in a 1-mL cuvette. The samples were left to incubate for 15 min, and then, 75 μ L of acetylthiocholine iodide (AChI) solution (16 mM) and 476 μ L of DTNB (3 mM), were added. The reaction was monitored for 5 min at 405 nm. Assays were run with a blank containing all the components except AChE, which was replaced by HEPES buffer. The velocities of the reaction were calculated as well as the enzyme activity. A control reaction was carried out using the sample solvent (methanol) in the absence of any tested compound, and it was considered as 100% activity. The percentage inhibition of the enzyme activity due to the presence of increasing test compound concentration was calculated by the following Eq. (1)

$$\%I = 100 - (v_i/v_o \times 100) \quad (1)$$

in which v_i is the initial reaction rate in the presence of inhibitor and v_o is the initial rate of the control reaction. The inhibition curves were obtained by plotting the percentage of enzymatic inhibition versus inhibitor concentration, and a calibration curve was obtained from which the linear regression parameters were obtained.

4.6. Inhibition of self-mediated and Cu(II)-induced A β (1–42) aggregation

Amyloid- β peptide (1–42) ($A\beta_{42}$) was purchased from Aldrich as a lyophilized powder and stored at -20 °C. The samples were treated with 1,1,1,3,3,3-hexafluoropropan-2-ol (HFIP) to avoid self-aggregation and reserved. HFIP pretreated $A\beta_{42}$ samples were resolubilized with a CH_3CN/Na_2CO_3 (300 μ M)/NaOH (250 μ M) (48.3:48.3:4.3, v/v/v) solvent mixture in order to have a stable stock solution. This $A\beta_{42}$ alkaline solution (500 μ M) was diluted in phosphate buffer (0.215 M, pH 8.0) to obtain a 40 μ M solution. Due to the hydrophobic nature of the compounds under study, they were first dissolved in

methanol (1 mg/mL) and then further diluted in phosphate buffer to a final concentration of 480 tM.

To study the A₃₄₂ aggregation inhibition, a reported method, based on the fluorescence emission of thioflavin T (ThT), was followed.^{16,28,29} It is based on the assumption that reduction of the ThT fluorescence, due to competition of the compounds for the peptide interaction, imply reduced A₃ aggregation. To study the effects of the compounds on copper-induced A_{β1-42} aggregation, solutions of Cu(II) (200 μM) in phosphate buffer (0.2 M, pH 8.0) were prepared from a CuCl₂ stock solution (0.015 M). The assay consisted on the incubation of A_{β1-42} (40 μM) with or without Cu(II) (40 μM) in phosphate buffer with or without the ligands (80 μM). The incubation was performed at 37° C, for 24 h, and for the control, a sample of the peptide was incubated under identical conditions but without the inhibitor. After incubation, the samples were added to a 96-well plate (BD Falcon) with 180 tL of 5 tM ThT in 50 mM glycine-NaOH (pH 8.5) buffer. Blank samples were prepared for each concentration in a similar way, devoid of peptide. After 5-min incubation with the dye, the ThT fluorescence was measured using a Spectramax Gemini EM (Molecular Devices) at the following wavelengths: 446 nm (excitation) and 485 nm (emission). The percent inhibition of aggregation due to the presence of the test compound was calculated by Eq. (2), in which IF_i and IF_0 corresponded to the fluorescence intensities, in the presence and the absence of the test

$$I\% = 100 - (IF_i/IF_0 \times 100) \quad (2)$$

compound, respectively, minus the fluorescence intensities due to the respective blanks. The reported values were obtained as the mean ± SEM of duplicate of two different experiments.

4.7. MAOs Inhibition

MAO activity was measured in 96-well plates (triplicate wells) by coupling the production of hydrogen peroxide is *via* horseradish peroxidase to a dye producing the fluorescent resorufin.^{35,45} Membrane-bound human MAO A and MAO B, horseradish peroxidase, and Ampliflu Red were obtained from Sigma-Aldrich (UK). For reversible inhibition, MAO was added last to the assay mixture containing (at final concentrations) 20 tM Ampliflu Red, 1 U/mL horseradish peroxidase, 1 mM tyramine. To see whether there was irreversible inhibition; MAO and inhibitor were preincubated in 100 tL

phosphate buffer pH 7.5 at 30 °C for 30 min before adding 100 μ L containing the rest of the assay components to start the reaction. Solubility limited the maximum concentration of inhibitor to 100 μ M. The data were analyzed in Graphpad PRISM 4 using the sigmoidal equation constrained to a bottom value of zero.

4.8. Cells and treatments

Human Neuroblastoma SH-SY5Y cell line was purchased from ATCC-CRL-2266. Briefly, the cells were grown in Dulbecco's modified Eagle's medium (DMEM) obtained from Gibco-Invitrogen (Life Technologies Ltd, UK) with 10% heat inactivated fetal calf serum, containing 50 U/mL penicillin, and 50 μ g/mL streptomycin, under a humidified atmosphere of 95% air- 5% CO₂ at 37 °C. Cells were plated at 0.1 X 10⁶ cells/mL for MTT cell proliferation assay. Medium was changed after 24 h and immediately before treatments.

The tested compounds (**10a**, **10b**, **10c**, **10d**, **10e**, **10f**, **10g**, **10h**) were dissolved in DMSO at a concentration of 25 mM and aliquots were stored at -20 °C. The compounds **10a**, **10d** and **10h** were added to the medium at 2.5 μ M final concentration; the compounds **10b**, **10c**, **10e**, **10f**, **10g** were added to the medium at 1 μ M final concentration; KC1 was added to the medium at 10 nM final concentration. The final concentration of DMSO in culture media did not exceed 0.05% (v/v) and no alterations on cells were observed. Cells were pre-incubated for 1 h with the compounds and then incubated with A₃₄₂ or H₂O₂ for another 24 h. A₃₄₂ was prepared as 276.9 μ M stocks in sterile water and added to the medium to 1 μ M final concentration. H₂O₂ was freshly prepared as 5 mM stocks in water and added to the medium to 100 μ M final concentrations. A₃₄₂ was purchased from American Peptide (Sunnyvale, CA, USA) and H₂O₂ from Sigma Chemical Co (St. Louis, MO, USA). For all conditions tested, control experiments were performed in which the compounds tested, A₃₄₂ or H₂O₂ were not added.

MTT cell proliferation assay

Cell proliferation was determined by the colorimetric MTT (3-(4,5-dimethylthiazol-2-yl)-2,5-diphenyltetrazolium bromide) assay.⁴⁶ In viable cells, MTT is metabolized into a formazan that absorbs light at 570 nm. Following the cell treatment protocol the medium was aspirated and 0.5 mL MTT (0.5 mg/ml) was added to each well. The plate was then

incubated at 37 °C for 3 h. At the end of the incubation period the formazan precipitates were solubilized with 0.5 mL of acidic isopropanol (0.04 M HCl/isopropanol). The absorbance was measured at 570 nm. Cell reduction ability was expressed as a percentage of the untreated cells.

All data result from the analysis of duplicates per experimental condition in at least three independent experiments and are expressed as the mean±SEM. Statistical analyses were performed using GraphPad Prism 5 (GraphPad Software, San Diego, CA, USA). Statistical tests between multiple data sets and conditions were carried out using a one-way analysis of variance (ANOVA) with pairwise multiple comparison procedures using the post hoc Bonferroni's test to determine statistical significance, as appropriate. A p value <0.05 was considered statistically significant.

Acknowledgements. The authors acknowledge the Portuguese *Fundação para a Ciência e Tecnologia* (FCT) for the project UID/QUI/00100/2013, postdoctoral fellowships (RSK and KC), and also the Portuguese NMR (IST-UL Center) and Mass Spectrometry Networks (Node IST-CTN) for providing access to their facilities. We also thank the doctoral fellowship from Erasmus Namaste program (AH) and P-L. Joffrin for his contribution to the MAO bioassays at the University of St Andrews.

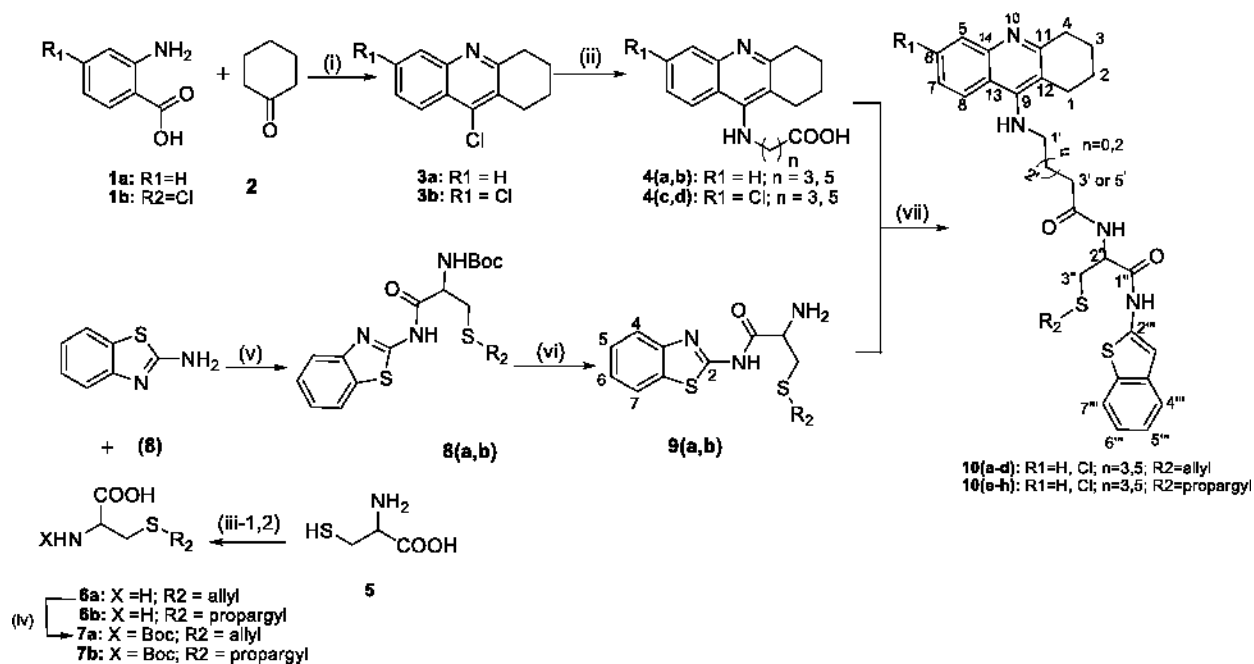
References

-
- ¹ Alzheimer's Association, *Alzheimer's Dement.*, 2014, 10, 47.
 - ² S. Oddo, A. Caccamo, J. D. Shepherd, M. P. Murphy, T. E. Golde, R. Kaye, R. Metherate, M. P. Mattson, Y. Akbari and F. M. LaFerla, *Neuron.*, 2003, 39, 409.
 - ³ S. Ayton, P. Lei and A. I. Bush, *Free Radical Biol. Med.*, 2013, 62, 76.
 - ⁴ J. L. Cummings, M. Travis and K. Zhong, *Alzheimer's Res. Ther.*, 2014, 6, 37.
 - ⁵ A. Cavalli, M. L. Bolognesi, A. Minarini, M. Rosini, V. Tumiatti, M. Recanatini and C. Melchiorre, *J. Med. Chem.*, 2008, 51, 347.
 - ⁶ H. Zheng, T. Amit, O. Bar-Am, M. Fridkin, M. B. H. Youdim and S. A. Mandel, *J. Alzheimer's Dis.* 2012, 30, 1.
 - ⁷ A. Mattevi, C. Binda, M. Li, F. Hubálek, *Curr. Med. Chem.*, 2004, 11, 1983.

-
- ⁸ M. B. Youdim, and J. J. Buccafusco, *Trends Pharmacol. Sci.*, 2005, 26, 27.
- ⁹ E. Nepovimova, E. Uliassi, J. Korabecny, L. E. Peña-Altamira, S. Samez, A. Pesaresi, G. E. Garcia, M. Bartolini, V. Andrisano, C. Bergamini, R. Fato, D. Lamba, M. Roberti, K. Kuca, B. Monti and M. L. Bolognesi, *J. Med. Chem.*, 2014, 57, 8576.
- ¹⁰ R. Leon, A.G. Garcia and J. Marco-Contelles, *Med. Res. Rev.*, 2013, 33, 139.
- ¹¹ G. Small and R. Bullock, *Alzheimer's Dement.*, 2011, 7, 177.
- ¹² M. L. Crismon, *Ann. Pharmacother.*, 1994, 28, 744.
- ¹³ A. Romero, R. Cacabelos, M. J. Oset-Gasque, A. Samadi and J. Marco-Contelles, *Bioorg. Med. Chem. Lett.*, 2013, 23, 1916.
- ¹⁴ R. S. Keri, C. Quintanova, S. M. Marques, A. R. Esteves, S. M. Cardoso and M. A. Santos, *Bioorg. Med. Chem.*, 2013, 21, 4559.
- ¹⁵ A. Nunes, S. M. Marques, C. Quintanova, D. F. Silva, S. M. Cardoso, S. Chaves, M. A. Santos, *Dalton Trans.*, 2013, 42, 6058.
- ¹⁶ C. Quintanova, R. S. Keri, S. M. Marques, M. G-Fernandes, S. M. Cardoso, M. L. Serralheiro, M. A. Santos, *Med. Chem. Comm.*, 2015, 6, 1969.
- ¹⁷ A. Dairam, R. Fogel, S. Daya and J. L. Limson, *J. Agric. Food Chem.*, 2008, 56, 3350.
- ¹⁸ J. M. Kim H. J. Chang, W. K. Kim, N. Chang and H. S. Chun, *J. Agric. Food Chem.*, 2006, 54, 6547.
- ¹⁹ R. S. Keri, C. Quintanova, S. Chaves, D. F. Silva, S. M. Cardoso and M. A. Santos, *Chem. Biol. Drug Des.* 2016, 87, 101.
- ²⁰ C. Quintanova, R. S. Keri, S. Chaves and M. A. Santos, *J. Inorg. Biochem.*, 2015, 151, 58.
- ²¹ C. Lu, Q. Zhou, J. Yan, Z. Du, L. Huang and X. Li, *Eur. J. Med. Chem.*, 2013, 62, 745.
- ²² S. Noel, S. Cadet, E. Gras and C. Hureau, *Chem. Soc. Rev.*, 2013, 42, 7747.
- ²³ H. Dvir, I. Silman, M. Harel, T. L. Rosenberry and J. L. Sussman, *Chem-Biol. Interact.* 2010, 187, 10.
- ²⁴ PDB, entry 1ODC. <http://www.rcsb.org/pdb/explore/explore.do?structureId=1ODC>.
- ²⁵ E. H. Rydberg, B. Brumshtein, H. M. Greenblatt, D. M. Wong, D. Shaya, L. D. Williams, P. R. Carlier, Y. Pang, I. Silman and J. L. Sussman, *J. Med. Chem.*, 2006, 49, 5491.
- ²⁶ L. J. Sargent and L. J. Small, *Org. Chem.*, 1946, 11, 359.
- ²⁷ M. K. Hu and C. F. Lu, *Tetrahedron Lett.*, 2000, 41, 1815.
- ²⁸ M. Bartolini, C. Bertucci, M. L. Bolognesi, A. Cavalli, C. Melchiorre and V. Andrisano, *Chem. BioChem.*, 2007, 8, 2152.

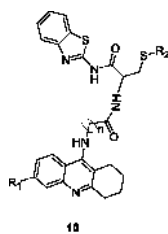
-
- ²⁹ X. Chao, X. He, Y. Yang, X. Zhou, M. Jin, S. Liu, Z. Cheng, P. Liu, Y. Wang, J. Yu, Y. Tan, Y. Huang, J. Qin and S. Rapposelli, *Bioorg. Med. Chem. Lett.*, 2012, 22, 6498.
- ³⁰ A. Hawe, M. Sutter, W. Jiskoot, *Pharm. Res.*, 2007, 25, 1487.
- ³¹ B. Tepe, D. Daferera, A. Sokmen, M. Sokmen and M. Polissiou, *J. Agric. Food. Chem.*, 2005, 90, 333.
- ³² Q. H. Gong, Q. Wang, L. L. Pan, X. H. Liu, H. Xin and Y. Z. Zhu, *Brain Behav. Immun.*, 2011, 25, 110.
- ³³ S. M. Denecke, *Curr. Top Cell Regul.*, 2000, 36, 151.
- ³⁴ M. J. Zhou, Z. J. Diwu, N. PanchukVoloshina and R. P. Haugland, *Anal. Biochem.*, 1997, 253, 162.
- ³⁵ G. Esteban, J. Allan, A. Samadi, A. Mattevi, M. Unzeta, J. Marco-Contelles, Claudia Binda, Rona R. Ramsay, *Biochim. Biophys. Acta, Proteins Proteomics*, 2014, 1844, 1104.
- ³⁶ QikProp, version 2.5, Schrödinger, LLC, New York, NY, 2005.
- ³⁷ C. A. Lipinski, F. Lombardo, B. W. Dominy and P. J. Feeney, *Adv. Drug Deliv. Rev.*, 1997, 23, 3.
- ³⁸ W. L. F. Armarego, D. D. Perrin, Purification of Laboratory Chemicals, 4th ed.; Butterworth-Heinemann: Oxford, 1999.
- ³⁹ E. H. Rydberg, B. Brumshtein, H. M. Greenblatt, D. M. Wong, D. Shaya, L. D. Williams, P. R. Carlier Y. Pang, I. Silman and J. L. Sussman, *J. Med. Chem.*, 2006, 49, 5491.
- ⁴⁰ Maestro, version 9.3. Schrödinger Inc.: Portland, OR, 2012.
- ⁴¹ T. Hassinen and M. J. Peräkylä, *Comput. Chem.*, 2001, 22, 1229.
- ⁴² M. Clark, R. D. Cramer III and N. Van Opdenbosch, *J. Comput. Chem.*, 2004, 10, 982.
- ⁴³ G. Jones, P. Willett, R. C. Glen, A. R. Leach and R. Taylor, *J. Mol. Biol.*, 1997, 67, 727.
- ⁴⁴ J. Sebestík, S. M. Marques, P. L. Falé, S. Santos, D. M. Arduíno, S. M. Cardoso, C. R. Oliveira, M. L. Serralheiro and M. A. Santos, *J. Enzyme Inhib. Med. Chem.*, 2011, 26, 485.
- ⁴⁵ R. R. Ramsay, A. Olivieri and A. Holt, *J. Neural Transm.*, 2011, 118, 1003.
- ⁴⁶ T. Mosmann, *J. Immunol. Methods*, 1983, 65, 55.

Scheme, Figs and tables



Scheme 1. Reagents and conditions (i) POCl₃, 180 °C, reflux, 3 h; (ii) 2 equiv H₂N(CH₂)_nCO₂H, phenol, KI, reflux, 4 h; (iii) allyl bromide (iii-1) or propargyl bromide (iii-2), NH₄OH (2M), r.t., 3 h; (iv) di-tert-butyl dicarbonate and Na₂CO₃, THF, r.t., 5 h; (v) 1.5 equiv T₃P, 2.5 equiv NMM, CH₂Cl₂, rt, 3 h; (vi) TFA, CH₂Cl₂, rt, 2 h; (vii) 1.5 equiv T₃P, 2.5 equiv NMM, CH₂Cl₂, r.t., 3 h;

Table 1. *In vitro* activities of the TAC-SAC–BTA and TAC-SPRC-BTA hybrids towards the inhibition of AChE and MAO enzymes and also A₃₄₂ aggregation (self- and Cu-induced).



Compound Code	R ₁	R ₂	n	AChE inhibition IC ₅₀ (μM) ^a	MAO A inhibition IC ₅₀ (μM) ^d	MAO B inhibition IC ₅₀ (μM) ^d	A ₃₄₂ self-aggr. inhib. (%) ^{b,c}	A ₃₄₂ Cu-induc. aggr. inhib. (%)
10a	H		3	0.365	16.2	63±8	57.8	-
10b	H		5	0.374			78.2	-
10c	Cl		3	0.280	10.8	55	31.6	56.6
10d	Cl		5	0.277			14.0	-
10e	H		3	0.348			77.2	-
10f	H		5	0.351			56.3	-
10g	Cl		3	0.248	27.7	85	24.1	37.6
10h	Cl		5	0.268	77.1	95	19.3	-
Tacrine	-	-	-	0.457			19.5	-
Clorgyline					0.42x10 ⁻³	10.6		

^a The values are mean of five independent experiments ± SD.

^b Inhibition of A₃₄₂ aggregation (in %) without and with copper (40 tM). The thioflavin-T fluorescence method was used, and the measurements were carried out in the presence of inhibitor (80 tM).

^c The values are the mean of two independent measurements in duplicate (SEM < 10%).

^d The values are the mean of two independent measurements each with 21 points (SEM < 15%).

Table 1S: Predicted pharmacokinetic values^a

S.No.	Comp. Code	R ₁	R ₂	MW	clog P ^b	log BB ^c	Caco-2 permeability (nm/sec)	Violations of Lipinski's rule of 5	CNS activity
1	10b	H		559.75	5.859	-1.355	590	2	--
2	10c	H		587.80	6.684	-1.550	613	2	--
3	10e	Cl		594.19	6.187	-0.740	1263	2	-
4	10f	Cl		622.24	7.366	-1.281	890	2	--
5	10h	H		557.73	5.786	-1.508	445	2	--
6	10i	H		585.78	6.671	-1.308	999	2	--
7	10k	Cl		592.17	6.231	-1.280	477	2	--
8	10l	Cl		620.23	6.918	-1.020	1350	2	--

^a Predicted values using program QikProp v. 2.5³⁴. ^b Calculated octanol/water partition coefficient. ^c Brain/blood partition coefficient.

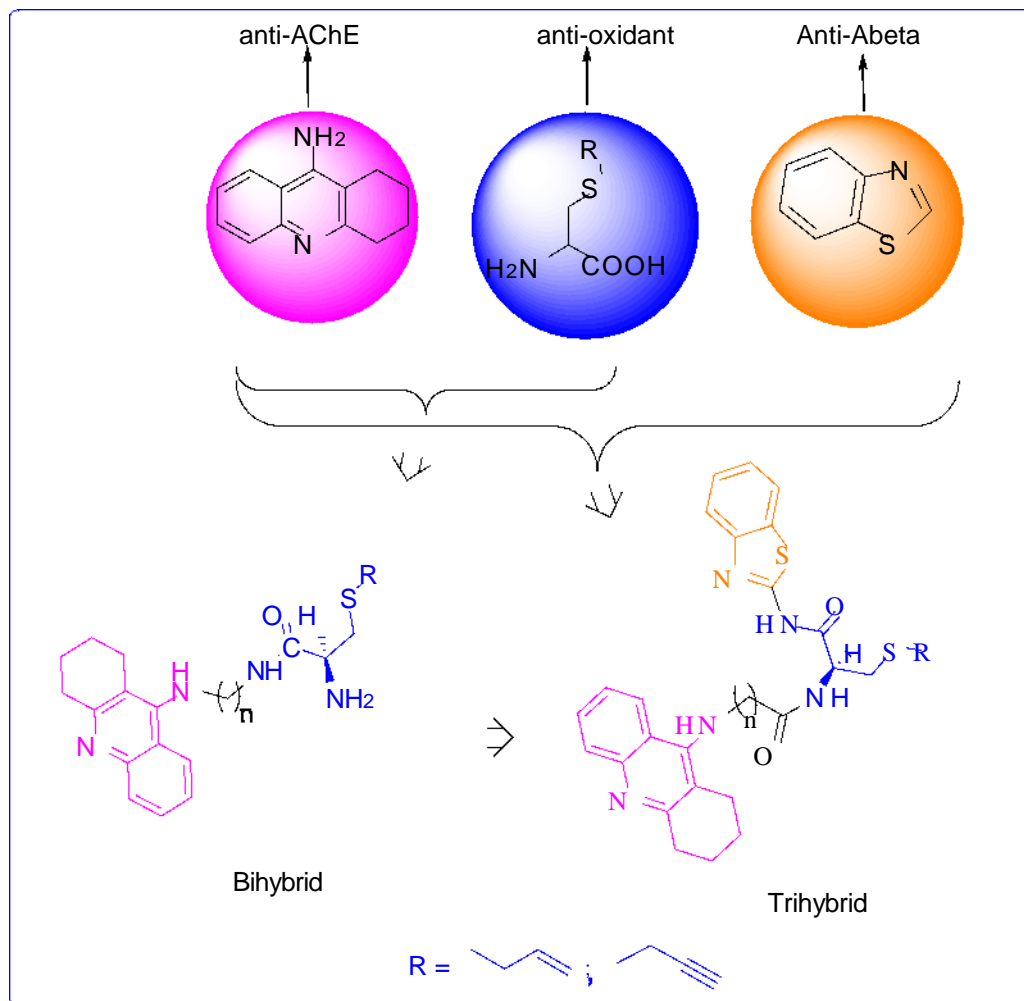
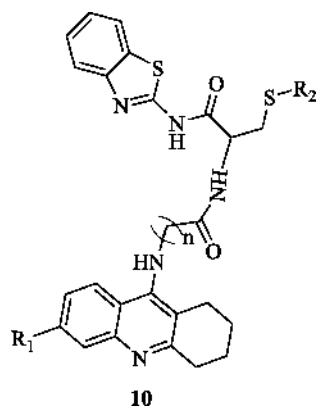


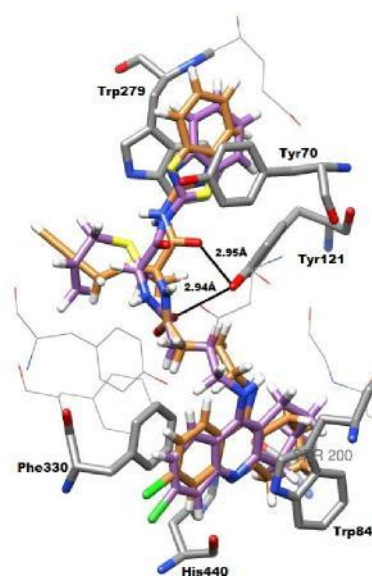
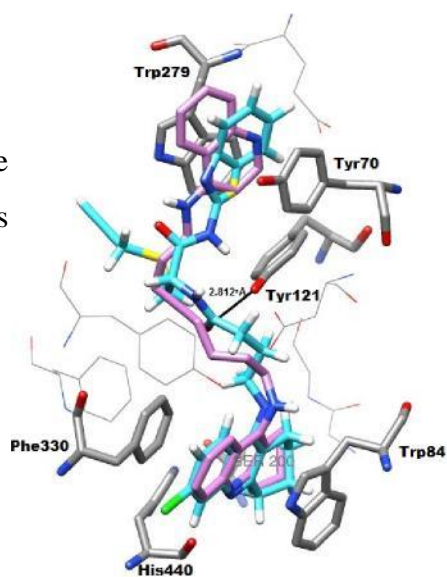
Figure 1: Design strategy for the novel trihybrids TAC-SAC-BTA and TAC-SPRC-BTA



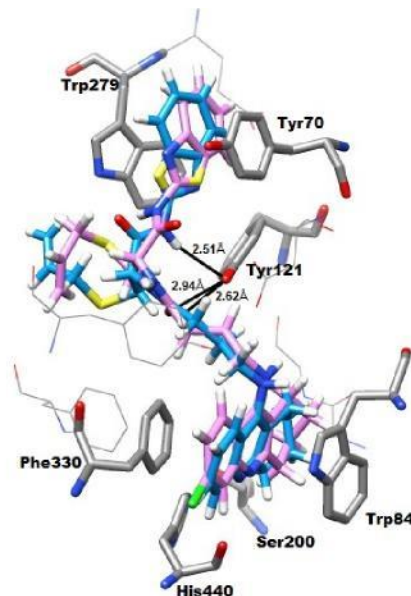
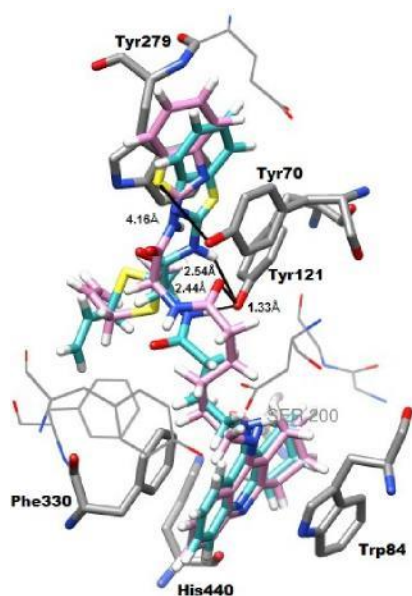
R_1	H	H	Cl	Cl	H	H	Cl	Cl
R_2								
n	3	5	3	5	3	5	3	5

Figure 2: Synthesized compounds: TAC-SAC-BTA ($R_2 =$ allyl) and TAC-SPRC-BTA ($R_2 =$ propargyl)

Figure
results
SAC-
TAC-



A
C
3: Docking
for the TAC-
BTA and
SPRC-BTA
trihybrids with
TcAChE: (A)



superimposition of the original ligand (PDB entry 1ODC) (pink) and 10g (cyan); (B) superimposition of 10c (purple) and 10g (brown); (C) superimposition of 10b (pink) and 10a (cyan); (D) superimposition of 10c (pink) and 10a (blue).

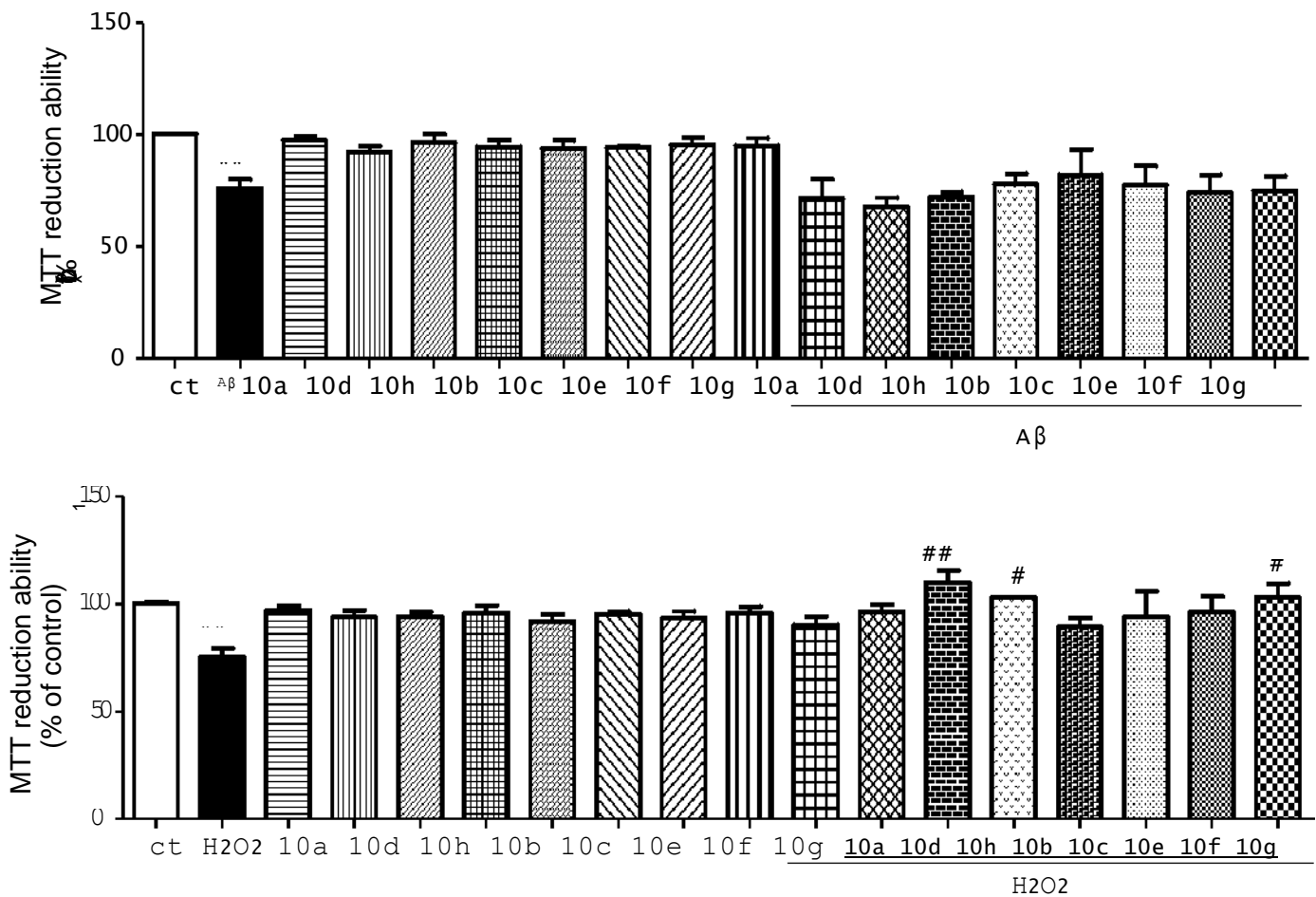


Figure 4. Effect of the described compounds on Aβ₄₂ peptide or H₂O₂ toxicity in SH-SY5Y cells. SH-SY5Y cells were treated with Aβ₄₂ (1 μM) or H₂O₂ (100 μM) for 24 h, in the absence or the presence of the compounds. Evaluation of cell viability was performed by using MTT reduction test. Results are expressed as the percentage of SH-SY5Y untreated cells, with the mean ± S.E.M. derived from 3 different experiments. **p < 0.01, significantly different when compared with SH-SY5Y untreated cells; #p < 0.05; ##p < 0.01, significantly different when compared with H₂O₂ treated cells.